0026-895X/98/030590-07$3.00/0

MOLECULAR PHARMACOLOGY, **53:**590–596 (1998).

Antagonist Properties of a Phosphono Isoxazole Amino Acid at Glutamate R1–4 (*R,S*)-2-Amino-3-(3-hydroxy-5-methyl-4-isoxazolyl)propionic Acid Receptor Subtypes

PHILIP WAHL, CHARLOTTE ANKER, STEPHEN F. TRAYNELIS, JAN EGEBJERG, JESPER S. RASMUSSEN, POVL KROGSGAARD-LARSEN, and ULF MADSEN

Department of Molecular Pharmacology, Novo Nordisk A/S, Novo Nordisk Park, DK-2760 Maaloev, Denmark (P.W., C.A.), Department of Pharmacology, Emory University, Atlanta, GA 30322-3090, USA (S.F.T.), Department of Molecular Genetics, Novo Nordisk A/S, DK-2880 Bagsværd, Denmark (J.E., J.S.R.) and Department of Medicinal Chemistry, The Royal Danish School of Pharmacy, DK-2100 Copenhagen, Denmark (P.K.-L., U.M.)

Received July 18, 1997; Accepted November 5, 1997

This paper is available online at http://www.molpharm.org

ABSTRACT

The activity of the (*R,S*)-2-amino-3-(3-hydroxy-5-methyl-4-isoxazolyl)propionic acid (AMPA) receptor antagonist, (*R,S*)-2-amino-3-[5-*tert*-butyl-3-(phosphonomethoxy)-4-isoxazolyl]propionic acid (ATPO), at recombinant ionotropic glutamate receptors (GluRs) was evaluated using electrophysiological techniques. Responses at homo- or heterooligomeric AMPA-preferring GluRs expressed in human embryonic kidney (HEK) 293 cells (GluR1-flip) or *Xenopus laevis* oocytes (GluR1–4-flop or GluR1-flop + GluR2) were potently inhibited by ATPO with apparent dissociation constants (K_b values) ranging from 3.9 to 26 μM. A Schild analysis for kainate (KA)-activated GluR1 receptors showed ATPO to have a K_B of 8.2 μM and a slope of unity, indicating competitive inhibition. The antagonism by ATPO at GluR1 was of similar magnitude at holding potentials between −100 mV and +20 mV. In contrast, ATPO (<300 μM), does not inhibit responses to kainate at homomeric GluR6 or heterooligomeric GluR6/KA2 expressed in HEK 293 cells but activated GluR5 and GluR5/KA2 expressed in *X. laevis* oocytes. ATPO produced <15% inhibition at the maximal concentration (300 μM) of current responses through NR1A + NR2B receptors expressed in *X. laevis* oocytes. Thus, ATPO shows a unique pharmacological profile, being an antagonist at GluR1–4 and a weak partial agonist at GluR5 and GluR5/KA2.

Receptors for the central excitatory neurotransmitter glutamate are the subject of extensive exploration as potential targets for drug intervention in different neurological disorders. Notably, antagonists at such receptors have the potential for treatment of a number of neurodegenerative disorders and epilepsies (Rogawski, 1993; Meldrum, 1994). Ionotropic GluRs have been subdivided on the basis of pharmacology and molecular structure into three classes: NMDA, AMPA, and KA receptors (Watkins *et al.*, 1990; Simon, 1992). The latter two mediate fast excitatory signals in the mammalian central nervous system and are often referred to as non-NMDA receptors because of the lack of antagonists that distinguish them. Such antagonists are indispensable tools for understanding the pharmacology and physiological functions of AMPA and KA receptors.

This work was supported by grants from the European Economic Community (BIO2-CT93-0243) and the John Merck Fund.

Molecular cloning experiments have revealed the existence of at least nine genes encoding non-NMDA receptor subunits (Keinänen *et al.*, 1990; Sommer *et al.*, 1992; Seeburg, 1993; Hollmann and Heinemann, 1994; Nakanishi and Masu, 1994). The AMPA-preferring receptors consist of homomeric or heteromeric combinations of the subunits GluR1–4. The KA-preferring receptors consist of the subunits GluR5–6 and KA1–2. GluR7 is a KA-preferring receptor, based on binding experiments. AMPA-preferring receptors can be activated by both AMPA and KA. The homomeric GluR6 receptor can be activated by KA but not AMPA, whereas heteromeric receptors containing GluR6 and KA2 can be activated by both AMPA and KA (Sommer *et al.*, 1990; Egebjerg *et al.*, 1991; Herb *et al.*, 1992).

A number of quinoxalinediones are widely used as antagonists at non-NMDA receptors, especially NBQX, which shows 5-fold selectivity for AMPA receptors over KA receptors (Sheardown *et al.*, 1990). AMOA is a rather weak non-

ABBREVIATIONS: AMOA, (*R*,*S*)-2-amino-3-[3-(carboxymethoxy)-5-methyl-4-isoxazolyl]propionic acid; AMPA, (*R*,*S*)-2-amino-3-(3-hydroxy-5-methyl-4-isoxazolyl)propionic acid; ATPO, (*R*,*S*)-2-amino-3-[5-*tert*-butyl-3-(phosphonomethoxy)-4-isoxazolyl]propionic acid; GluR, glutamate receptor; HEK, human embryonic kidney; KA, kainate; NBQX, 2,3-dihydroxy-6-nitro-7-sulfamoylbenzo(*f*)quinoxaline; NMDA, *N*-methyl-D-aspartate; NR1, *N*-methyl-D-aspartate receptor subunits 1; NR2, *N*-methyl-D-aspartate receptor subunits 2; BAPTA, 1,2-bis(2-aminophenoxy)ethane-*N*,*N*,*N*′,*N*′-tetraacetic acid; HEPES, 4-(2-hydroxyethyl)-1-piperazineethanesulfonic acid.

NMDA antagonist showing some selectivity for AMPA receptors (Krogsgaard-Larsen *et al.*, 1991; Wahl *et al.*, 1992). Recently, LY293558 [(3*S*,4a*R*,6*R*,8a*R*)-6-[2-(1(2)*H*-tetrazol-5-yl)ethyl]decahydroisoquinoline-3-carboxylate] has been shown to block responses at GluR5- and AMPA-preferring receptors, leaving responses at GluR6 relatively unaffected (Bleakman *et al.*, 1996). In addition to these competitive antagonists, 2,3-benzodiazepines such as 1-(4-aminophenyl)-3-methylcarbamyl-4-methyl-7,8-methylenedioxy-3,4-dihydro-5*H*-2,3-benzodiazepine act as noncompetitive antagonists with selectivity toward AMPA-preferring receptors (Wilding and Huettner, 1995).

In this study, we describe the pharmacology of the new AMPA receptor antagonist ATPO (Madsen *et al.*, 1996) by comparing effects of ATPO on currents through homo- and heterooligomeric AMPA- and KA-preferring GluRs expressed in *Xenopus laevis* oocytes and mammalian cell lines. Inhibition curves and Schild analysis have been performed with ATPO, and a series of comparative pharmacological studies on ATPO and AMOA is reported. Our results indicate that ATPO has a unique pharmacological profile, being a potent competitive antagonist of AMPA-preferring receptors (GluR1–4) devoid of activity at GluR6 and GluR6/KA2 and with slight agonist activity at GluR5 and GluR5/KA2.

Materials and Methods

Tissue culture and cDNA transfection. HEK 293 cells (American Type Culture Collection, Rockville, MD) were plated on 12-mm glass coverslips coated with poly-D-lysine (0.1–0.6 mg/ml) and maintained in standard Dulbecco's modified Eagle's medium supplemented with 10% fetal calf serum and penicillin/streptomycin. HEK 293 cells were transiently transfected with 0.1–1.0 μg/ml GluR1-flip, GluR6(Q), or GluR6(Q) + KA2 cDNA in cytomegalovirus-based mammalian expression vectors (KA2 was provided by J. Boutler, Salk Institute, La Jolla, CA). The reporter gene CD8 [0.2–0.6 μg/ml; provided by B. Seed; antibody-coated microbeads were from Dynal (Oslo, Norway)] was used to identify individually transfected cells.

Fast drug application. The fast application of glutamate to cells for 100–200 msec was performed using a piezobimorph-driven double-barreled perfusion system. Flow in each side of θ tubing was controlled by a solenoid valve, and a rotary valve was used to switch between different solutions in each barrel. The agonist barrel was preflushed for 1–4 sec to remove any dilute solution at the tip, and 100 V subsequently applied to the piezobimorph to move the perfusion pipette so that the cell was placed in the agonist stream. Application of antagonists was performed 30–40 sec before coapplication of antagonist plus glutamate to allow equilibration.

Electrophysiology on mammalian cells. Currents were recorded on either an Axopatch 200A (Axon Instruments, Foster City, CA) or a List EPC-9 (HEKA Electronic GmbH, Lambrecht, Germany) amplifier. All experiments were performed at 20–23°, and the holding potential was between −40 and −60 mV. External recording solution for all experiments was 150 mM NaCl, 3 mM KCl, 1 mM $CaCl_2$, 1 mM $MgCl_2$, 20 mM mannitol, 10 mM HEPES, pH 7.4. The internal solution was composed of 110 mM D-gluconic acid, 110 mM CsOH, 30 mM CsCl, 0.5 mM $CaCl_2$, 2 mM $MgCl_2$ 4 mM NaCl, 5 mM BAPTA, 2 mM Na-ATP, 0.3 mM Na-GTP, 5 mM HEPES, pH 7.3, using CsOH; osmolality was 330 mOsmol. Experiments on GluR6-expressing baby hamster kidney cells were performed after preincubation in buffer containing concanavalin A (250 μg/ml, Type IV; Sigma, St. Louis, MO) for 5–10 min to prevent agonist-induced desensitization (Egebjerg *et al*., 1991).

Preparation of RNA. Plasmids containing NR1A and NR2B were kindly provided by Professor S. Nakanishi (Kyoto University, Japan). *In vitro* transcripts from GluR1-flip, GluR3-flip, GluR4-flip, GluR2, NR1A, and NR2B were made using an mRNA capping kit (Strategene, La Jolla, CA) after linearization of CsCl gradient-purified DNA. cRNA transcripts were extracted with phenol/chloroform (1:1) and chloroform/isoamyl alcohol (24:1) and purified by precipitation in ammonium acetate and ethanol. RNA was dissolved in diethyl pyrocarbonate-treated water.

***X. laevis* oocyte expression system.** Mature female *X. laevis* obtained from Xenopus I (Ann Arbor, MI) were anesthetized using 0.15% ethyl 3-aminobenzoate (MS-222), and three to five ovarian lobes were surgically removed. Oocytes at developmental stages V–VI were dissected from the ovary and injected with 5–20 ng of cRNA using pipets with a tip diameter of 20–30 μm. For expression of heteromeric combinations, a 1:4 ratio of GluR1 to GluR2 or a 1:2 ratio of NR1A to NR2B cRNA was used. Oocytes were stored in Barth's medium containing 88 mM NaCl, 1 mM KCl, 2.4 mM $NaHCO_3$, 0.3 mM $Ca(NO_3)_2$, 0.41 mM $CaCl_2$, 0.82 mM $MgSO_4$, 15 mM HEPES, pH 7.4, and supplemented with 0.1 mg/ml gentamycin sulfate. Two days after injection, the oocytes were treated with 0.5 mg/ml collagenase for 20–30 min, and the follicle cell layer was removed mechanically with a pair of fine forceps. Recordings were performed using a Turbo TEC 01C (NPI Electronic GmBH, Tamm, Germany) two-electrode voltage clamp, over periods ranging between 3 and 8 days after injection. Current and potential measuring electrodes were filled with 3 M KCl, and the pipette resistances were 0.5–1.0 MΩ. The oocytes were placed in a small plexiglass chamber that was continuously perfused (3 ml/min) with frog Ringer's solution containing 115 mM NaCl, 2 mM KCl, 1.8 mM $CaCl_2$, and 5 mM HEPES, pH 7.2. Drugs were applied through the bath solution. Experiments on GluR5- and GluR5/KA2-expressing oocytes were performed after preincubation in Ringer's solution containing concanavalin A (500 μg/ml, Type IV; Sigma) for 5–10 min to prevent agonist-induced desensitization (Egebjerg *et al*., 1991).

Data analysis. Agonist concentration-response curves were produced by measuring the maximal current induced by increasing concentrations of agonist. Data from individual oocytes were fitted to the logistic equation (De Lean *et al.*, 1978):

$$I = I_{max}/\{1 + (EC_{50}/[agonist])^n\} \quad (1)$$

where I is the current induced by the agonist. The parameters I_{max} (maximal current at infinite agonist concentration), n (the Hill coefficient), and EC_{50} (concentration of agonist producing a current 50% of I_{max}) were determined by an iterative least-squares fitting routine (Origin; MicroCal Software, Northampton, MA). The IC_{50} values were determined by fitting the data to eq. 1, except that EC_{50} was replaced with IC_{50}, n was negative, and I_{max} was the current evoked by agonist alone. The K_b values for ATPO were determined from inhibition curves using the Leff-Dougall equation (Leff and Dougall, 1993):

$$K_b = IC_{50}/\{\{2 + ([agonist]/EC_{50})^b\}^{1/b} - 1\} \quad (2)$$

where [agonist] is the fixed concentration of agonist used to construct the inhibition curve, EC_{50} is the half-maximal agonist concentration, and b is the slope factor of the concentration-response relationship. Unless otherwise stated, all data quoted in the text are given as mean ± standard errors of at least three experiments.

Drugs ATPO was synthesized as previously described (Madsen et al., 1996). AMOA and AMPA were purchased from Research Biochemicals International (Natick, MA), KA and concanavalin A were from Sigma, and NBQX was synthesized at Novo Nordisk A/S (Copenhagen, Denmark).

Results

X. laevis oocytes expressing homomeric GluR1, GluR3, GluR4, or heteromeric combinations of GluR1 and GluR2 (GluR1/2) responded reproducibly to application of KA,

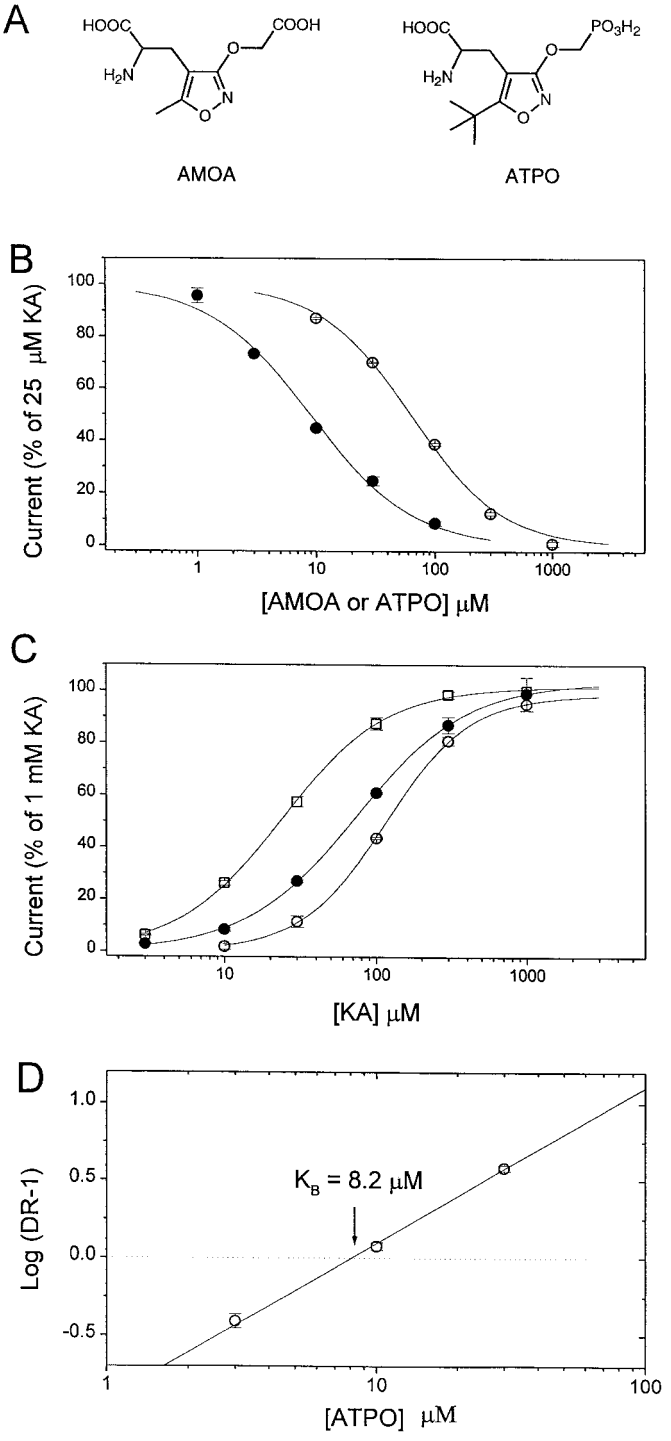

Fig. 1. Competitive inhibition by ATPO and AMOA of GluR1. A, Structures of ATPO and AMOA. B, Concentration-inhibition curves comparing potencies of ATPO (●) and AMOA (○) at GluR1-flop expressed in *X. laevis* oocytes. KA was used at 25 μM, and data are plotted as the mean ± standard error (n = 3–5) expressed as a fraction of control responses. *Smooth curves*, best fit of eq. 1 to the data for each antagonist. IC_{50} values and slope values are given in Tables 1 and 2. *C*, Concentration-response curves for KA (□) in the presence of 10 μM ATPO (■) or 150 μM AMOA (○) at GluR1 expressed in *X. laevis* oocytes. *Smooth curves*, best fit of eq. 1 to the data for each antagonist. The EC_{50} value was 24.2 ± 1.5 μM for KA alone, 67.2 ± 4.0 and 105 ± 11.3 μM for KA in the presence of 10 μM ATPO or 150 μM AMOA, respectively. D, Schild regression performed on *X. laevis* oocytes expressing GluR1 with KA as an agonist and ATPO as an antagonist. *Points*, mean ± standard error of dose-ratios (*DR*) from all experiments; *line,* results of linear regression through the pooled data points. The slope of the regression is 1.0.

TABLE 1

Agonist and antagonist pharmacology of recombinant AMPA receptors

Analysis of concentration-response experiments obtained for oocytes. EC_{50} values and Hill coefficients are from the best fits of the data to eq. 1 (see Materials and Methods).

Subtype	KA	AMPA	Glutamate
GluR1/2			
EC_{50} (μM)	134 ± 6.5	3.5 ± 0.58	17 ± 3.2
Hill coefficient	1.4 ± 0.04	1.8 ± 0.24	1.1 ± 0.09
GluR1			
EC_{50} (μM)	24 ± 1.5	2.3 ± 0.66	14 ± 0.89
Hill coefficient	1.3 ± 0.05	0.57 ± 0.02	1.4 ± 0.13
GluR3			
EC_{50} (μM)	53 ± 9.3		
Hill coefficient	1.3 ± 0.04		
GluR4			
EC_{50} (μM)	34 ± 4.5		
Hill coefficient	1.1 ± 0.06		

TABLE 2

Agonist and antagonist pharmacology of recombinant AMPA receptors

Analysis of concentration-inhibition experiments. IC_{50} values and Hill coefficients are from the best fit of the data to eq. 1. K_b values were estimated using a Leff-Dougall approach (see Materials and Methods).

Subtype	Agonist	Antagonist	IC_{50}	Hill coef.	K_b
			μM		μM
GluR1	AMPA (1 μM)	AMOA	253 ± 25	1.1 ± 0.1	57
GluR1	KA (25 μM)	AMOA	62 ± 3.9	1.2 ± 0.08	44
GluR1/2	KA (25 μM)	AMOA	97 ± 3.4	1.5 ± 0.03	76
GluR1	AMPA (1 μM)	ATPO	22 ± 1.8	0.71 ± 0.04	4.9
GluR1	KA (25 μM)	ATPO	5.3 ± 0.8	0.82 ± 0.04	3.9
GluR1/2	KA (25 μM)	ATPO	6.6 ± 0.21	1.2 ± 0.04	5.2
GluR1/2	Glu (10 μM)	ATPO	10 ± 0.66	0.90 ± 0.3	7.9
GluR3	KA (20 μM)	ATPO	12 ± 0.38	1.2 ± 0.1	15
GluR4	KA (20 μM)	ATPO	34 ± 2.8	0.96 ± 0.04	26

AMPA, and glutamate. Dose concentration experiments from oocytes expressing GluR1 showed that AMOA inhibited the sustained steady state current elicited by KA with an K_b of 44 μM (Fig. 1B; Tables 1 and 2). The rather weak potency of AMOA was compared with the potency of the *tert*-butylphosphonic acid analog, ATPO, which inhibited GluR1 with a K_b of 3.9 μM (Fig. 1). The potency of ATPO was somewhat lower at GluR3 (K_b = 14 μM) and GluR4 (K_b = 26 μM). Furthermore, because most AMPA receptors are heterooligomeric assemblies containing the GluR2 subunit, the effects of AMOA and ATPO were investigated on GluR1/2-expressing oocytes. The potency pattern was very similar for KA-induced GluR1/2 currents: ATPO showed highest affinity (K_b = 5.2 μM) and AMOA lowest affinity (K_b = 75.6 μM). Furthermore, using glutamate as the agonist, the K_b for ATPO was estimated to 7.9 μM (Tables 1 and 2).

The mechanism of inhibition was investigated by measuring effects of a fixed concentration of AMOA or ATPO on KA concentration-response relationships. At GluR1, 150 μM AMOA or 10 μM ATPO produced a 3–4-fold parallel leftward shift of the concentration-response curve for KA, which is consistent with competitive interaction (Fig. 1C). As a more stringent test of inhibitory mechanism, a Schild analysis for ATPO at GluR1 was performed (Fig. 1D). Schild regression plot of dose ratios versus ATPO concentration had a slope of 1.0, and the K_B was 8.2 μM. This result is consistent with the K_b value for ATPO calculated from concentration-inhibition curves.

The voltage dependence of ATPO effects at GluR1 was assessed by comparing levels of inhibition at three holding

TABLE 3

Effect of ATPO on recombinant kainate receptors

Whole-cell currents were recorded from cells transfected with GluR6 or GluR6/KA2. $I_{Glu+ATPO}/I_{Glu}$ is the ratio of the peak current to 300 μM glutamate and the peak current to 300 μM glutamate plus 300 μM ATPO. t_{DECAY} and the steady-state current were determined by fitting the data with amplitude (t) = $\text{amplitude}_{max}e^{(-t/t_{DECAY})}$ + baseline. n is the number of cells for all measurements.

	10–90% Rise		t_{DECAY}		$I_{Glu+ATPO}/I_{Glu}$	n
	Control	ATPO	Control	ATPO		
	msec					
GluR6	2.35 ± 0.08	2.46 ± 0.13	7.16 ± 0.61	7.17 ± 0.65	1.02 ± 0.03	7
GluR6/KA2	4.17 ± 0.28	3.83 ± 0.47	13.1 ± 1.60	10.7 ± 1.35	1.00 ± 0.04	8

TABLE 4

Currents recorded from oocytes injected with GluR5 or GluR5/KA2

Currents are normalized to the current elicited by KA. Data are normalized to the response elicited by 20 μM KA and the data are means of current responses from four to six oocytes.

	KA (20 μM)	AMPA (1 mM)	ATPO (50 μM)	AMOA (1 mM)
GluR5	1.0	0	0.15 ± 0.01	0
GluR5/KA2	1.0	0.39 ± 0.04	0.11 ± 0.02	0

potentials, −100 mV, −60 mV, and +20 mV. When tested against responses elicited by 25 μM KA, 10 μM ATPO caused 65.7 ± 2.5% inhibition at −100 mV, 65.9 ± 2.1% inhibition at −60 mV and 63.7 ± 2.8% inhibition at +20 mV (n = 4; data not shown).

One complicating factor in the above experiments is the slow rate of solution exchange that is possible in the *X. laevis* oocyte preparation, which limits the analysis of rapidly desensitizing responses at both AMPA- and KA-preferring recombinant receptors. To examine the actions of ATPO on the fast components of the glutamate-activated current responses at these receptors, HEK 293 cells were transfected with GluR1, GluR6, or GluR6/KA2, and glutamate was applied using a double-barreled piezobimorph-driven perfusion system. This drug application system permits us to investigate the action of ATPO on a time scale similar to that of postsynaptic events. Preequilibrium of ATPO was achieved by applying ATPO 20–30 sec before glutamate + ATPO. Coassembly of GluR6 and KA2 subunits was verified by applying 1 mM AMPA, because activation of GluR6 receptors by AMPA requires KA2 (Herb *et al*., 1992). Furthermore, the kinetics of GluR6/KA2 were significantly slower than those of homomeric GluR6 (Tables 3 and 4). Concentration-response experiments showed that glutamate activated both GluR1 (data not shown) and GluR6 (Traynelis and Wahl, 1997) with an EC_{50} value of about 0.5 mM, and therefore a concentration of 300 μM glutamate was used to determine the actions of ATPO. Concentration inhibition curves showed that the potency of ATPO (IC_{50} = 2.5 μM) at the GluR1 peak current was similar to the affinity of ATPO for the GluR1 steady state current described above (Fig. 1; Tables 1 and 2). At concentrations up to 300 μM, ATPO had no effect on the glutamate-activated peak current at GluR6 or heterooligomeric GluR6/KA2 combinations (Fig. 2; Tables 3 and 4). The rate of activation and desensitization was also unaffected by ATPO (Tables 3 and 4) Using the lower 95% confidence interval limits for the glutamate-activated current we calculated the lowest IC_{50} value, that would give a detectable difference when ATPO was applied at 300 μM, to be 4.1 and 3.2 mM for GluR6 and GluR6/KA2, respectively. This corresponds to a 500- and 390-fold selectivity toward inhibition of GluR1 (K_B value of 8.2 μM obtained from oocyte experiments) compared with GluR6 and GluR6/KA2, respectively (Fig. 3).

The potency of AMOA on GluR6 was assessed using baby hamster kidney cells stably expressing GluR6. After concanavalin A treatment of cells, application of 2–5 μM KA elicited robust nondesensitizing current responses. The cur-

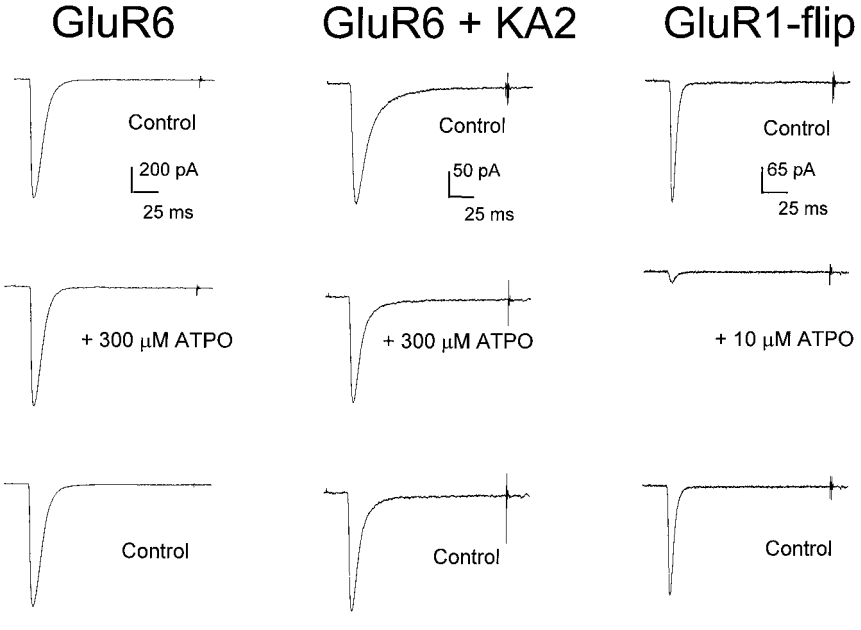

Fig. 2. Whole-cell responses induced by fast application of glutamate in HEK 293 cells expressing GluR6, GluR6/KA2, or GluR1-flip. To achieve rapid application of agonist, cells were lifted from the bottom of a coverslip into solutions flowing through barrels of a θ tubing pipette attached to a piezoelectric element moving the cell bathed in control solution to 150-msec pulses of agonist solution. The time course of solution exchange was estimated by open tip junction potential measurements to be 0.2–0.4 msec. Responses are shown before application, during the concomitant application of ATPO, and after ATPO washout. ATPO was present in the control solution 20–30 sec before ATPO plus glutamate was applied.

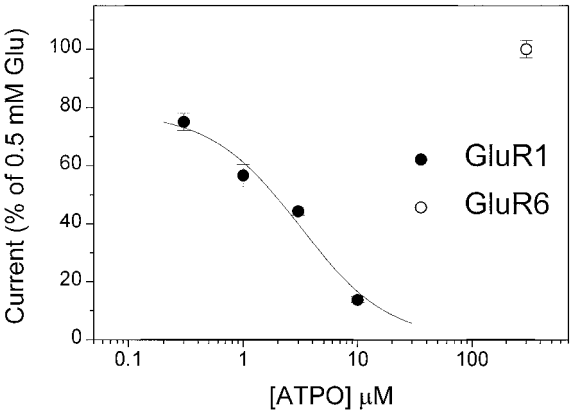

Fig. 3. ATPO inhibits responses at GluR1-flip (●) in a concentration-dependent manner, but has no effect on responses at GluR6 (○). Inhibition of the peak current induced by rapid application of 0.5 mM glutamate plotted against the concentration of ATPO. *Points*, data pooled from three to eight experiments; *vertical bars*, mean ± standard error; *Smooth curve*, best fit of eq. 1 to the data.

rent elicited by KA was virtually unaffected by either 500 μM AMOA (4.3 ± 2.0% inhibition, $n = 4$) or 300 μM ATPO (1.3 ± 2.4% inhibition, $n = 3$). In contrast, KA responses were sensitive to inhibition by 10 μM NBQX (75 ± 4% inhibition, $n = 3$) (data not shown). Similar results for the blocking action of NBQX at GluR6 has been reported previously by Bleakman *et al.* (1996), who determined an IC_{50} of 2.8 μM for NBQX against 1 μM KA.

The effect of ATPO was investigated on GluR5 expressed in

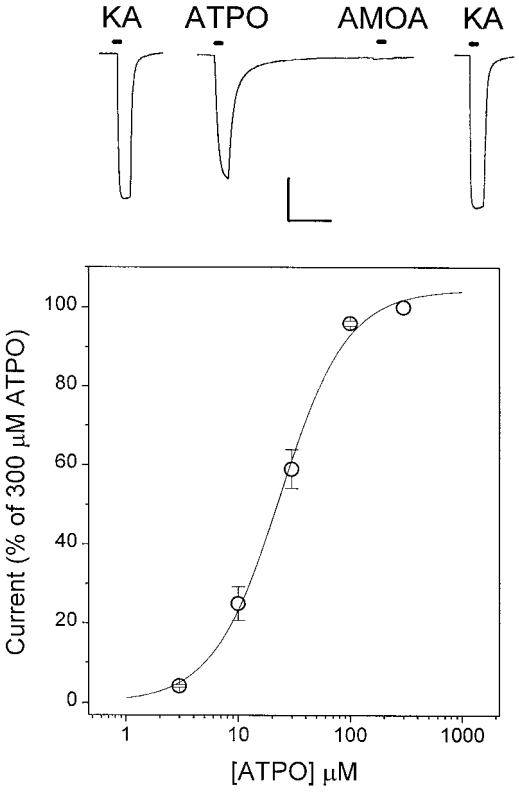

Fig. 4. *Top*, Sample records illustrating currents elicited by KA (20 μM), ATPO (50 μM), and AMOA (1 mM) from an oocyte expressing GluR5. *Scale*, 1 min and 200 nA (KA) or 20 nA (ATPO and AMOA). *Bottom*, Concentration-response curve for ATPO-induced GluR5 currents; *smooth curve*, best fit of eq. 1 to the data pooled from four oocytes.

X. laevis oocytes. As shown in Fig. 4, ATPO evoked inward currents (EC_{50} = 24 ± 3.3 μM) as did KA (EC_{50} = 16.2 μM) (16). The efficacy of ATPO and AMOA were examined by measuring current responses elicited by fixed concentrations of agonists from individual oocytes expressing GluR5 or GluR5/KA2. At homomeric GluR5, responses elicited by 50 μM ATPO were 6.6-fold smaller in amplitude compared with those elicited by 20 μM KA (Tables 3 and 4). In contrast, 1 mM AMOA elicited no current responses. Similar results were obtained for GluR5/KA2, except that AMPA elicited responses, indicating expression of heteromeric complexes (Tables 3 and 4).

The antagonist effects of ATPO and AMOA were also investigated at the NMDA receptor subunits NR1A + NR2B expressed in oocytes. As shown in Fig. 5, 300 μM ATPO produced marginal (<15%), inhibition when NMDA receptors were activated by 100 μM NMDA + 10 μM glycine. In contrast, 1000 μM AMOA caused about 50% inhibition. The mechanism of inhibition produced by AMOA seemed to be noncompetitive, because raising either the concentration of NMDA or glycine 10-fold had no effect (Fig. 5).

Discussion

The pharmacology of a newly developed AMPA receptor antagonist, ATPO, at recombinant GluR is described. ATPO has previously been shown to produce highly selective antagonism toward AMPA responses in an *in vitro* electrophysiological model using rat cortical tissue (Madsen *et al.*, 1996). Pharmacological and physiological characterization of AMPA and KA receptors have previously been performed using a variety of agonists and antagonists showing different degrees of selectivity (Fletcher and Lodge, 1996; Verdoorn, 1997). Quinoxalinediones have attracted much interest since their introduction as selective non-NMDA antagonists (Sheardown *et al.*, 1990; Watkins *et al.*, 1990). Subsequently, these molecules have been shown also to have affinity for the glycine binding site at NMDA receptors, and more importantly, quinoxalinediones such as NBQX only partially discriminate between AMPA- and KA-preferring receptors (Huettner, 1990; Egebjerg *et al.*, 1991; Nakanishi and Masu, 1994; Bleakman *et al.*, 1996). The noncompetitive AMPA/KA receptor antagonist Evans blue, which is a polycyclic diazo dye, has been described to be subunit specific (Keller *et al.*, 1993), but others have found it to be less selective (Price and Raymond, 1996). Recently, LY293558 has been reported as a potent and selective antagonist for GluR5- and AMPA-preferring receptors with no affinity for GluR6 (Bleakman *et al.*, 1996). A very important finding of the present study is that ATPO displays very high antagonist potency at the recombinant AMPA-preferring receptors (GluR1–4) compared with the potency at KA-preferring receptors (GluR6 and GluR6/KA2), and ATPO was found to be virtually inactive at NMDA receptors. The AMPA receptor antagonist AMOA (Krogsgaard-Larsen *et al.*, 1991), which is structurally related to ATPO, also showed AMPA receptor selectivity, but with approximately 10-fold lower potency and significant noncompetitive antagonist effects at NMDA receptors. ATPO showed partial agonist activity when tested at GluR5 expressed in *X. laevis* oocytes. ATPO and KA are equipotent at GluR5 though the efficacy of ATPO was considerably lower than that of KA.

GluR6 as well as complexes of GluR6 with KA2 form func-

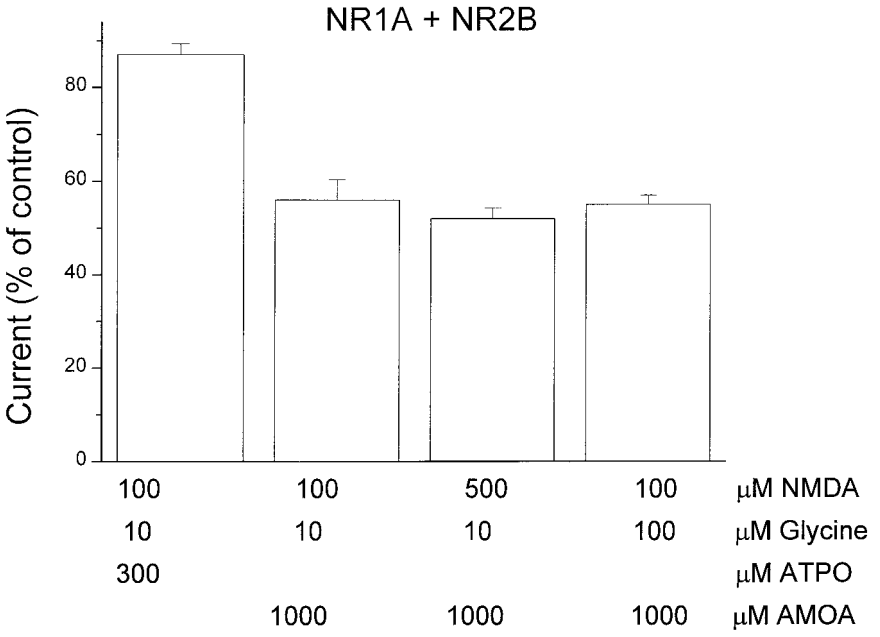

Fig. 5. Effect of ATPO and AMOA on NR1A + NR2B expressed in *X. laevis* oocytes. The bar graph shows the average (mean ± standard error) current expressed as a percentage of the current induced by NMDA plus glycine in the absence of antagonist. BAPTA (final concentration 1 mM) was injected 1 hr before recording, to prevent any activation of calcium-dependent chloride currents.

tional ion channels. In contrast to GluR6, GluR6/KA2 receptors are activated by AMPA (Herb *et al.*, 1992), and given the structural relationship between ATPO and AMPA, it was important to test whether these receptors were sensitive to ATPO. Our experiments indicated that, unlike NBQX, ATPO had no effect on currents through either subunit combination. This observation is important because *in situ* hybridization studies have demonstrated that the mRNA coding for GluR6 and KA2 colocalize in brain areas such as the cerebellar granule cell layer and caudate putamen (Herb *et al.*, 1992).

In terms of actual affinity, a Schild analysis for ATPO at GluR1 revealed a K_B of 8.2 μM in oocyte experiments using KA as an agonist. This result is in agreement with the IC_{50} value (2.5 μM) for ATPO obtained using rapid application of glutamate- to GluR1-expressing HEK 293 cells [for a detailed discussion on estimation of K_b values, see Lew and Angus (1995)]. The KA-elicited current through GluR1 expressed in oocytes was inhibited with the same potency as the current elicited by AMPA. Furthermore, the K_b for ATPO was not influenced significantly by coexpression of GluR1 and GluR2 in oocyte experiments.

In conclusion, ATPO has been shown to have a unique pharmacological profile at recombinant AMPA- and KA-preferring receptors. ATPO has a high antagonist potency at GluR1–4 and is very selective at the same receptors compared with the KA-preferring GluR6 and GluR6/KA2. In contrast to this finding, ATPO was also shown to be an agonist at GluR5 and GluR5/KA2 receptors. The latter activity is interesting in relation to a very recent letter in *Nature* (Clarke *et al.*, 1997), describing the AMPA agonist (*R*,*S*)-2-amino-3-(5-*tert*-butyl-3-hydroxy-4-isoxazolyl)propionic acid to be a potent agonist at GluR5. (*R*,*S*)-2-amino-3-(5-*tert*-butyl-3-hydroxy-4-isoxazolyl)propionic acid and ATPO show agonist versus antagonist activity at AMPA receptors, respectively, whereas they have similar agonist activity at GluR5. The two compounds share a *tert*-butyl substituent as a structural element, and this is in contrast to the close structural analogues AMPA and AMOA, which do not show activity at GluR5. The unique pharmacological profile of ATPO may be of value for further pharmacological studies of the receptor subtypes, and further structure-activity studies may shed light on the differences in profiles observed for AMPA, AMOA, ATPO, and other analogues. In particular, the activity profile of ATPO should prove extremely useful for dissecting out the relative contribution of AMPA and KA receptors to glutamate receptor responses in brain regions with low GluR5 expression.

References

Bleakman D, Schoepp DD, Ballyk B, Bufton H, Sharpe EF, Thomas K, Ornstein PL, and Kamboj RK (1996) Pharmacological discrimination of GluR5 and GluR6 kainate receptor subtypes by (4*S*,4a*R*,6*R*,8a*R*)-6-[2-(1(2)-tetrazole-5-yl)ethyl]decahydroisoquinoline-3 carboxylic acid. *Mol Pharmacol* **49**:581–585.

Clarke VJR, Ballyk BA, Hoo KH, Mandelzys A, Pellizzari A, Bath CP, Thomas J, Sharpe EF, Davies CH, Ornstein PL, Schoepp DD, Kamboj RK, Collindrige GL, Lodge D, and Blackman D (1997) A hippocampal GluR5 kainate receptor regulating inhibitory synaptic transmission. *Nature (Lond)* **389:**599–602.

De Lean A, Munson PJ, and Rodbard D (1978) Simultaneous analysis of families of sigmoidal curves: Application to bioassay, radioligand assay, and physiological dose-response curves. *Am J Physiol* **235**:E97–E102.

Egebjerg J, Bettler B, Hermans-Borgmeyer I, and Heinemann S (1991) Cloning of a glutamate receptor subunit activated by kainate but not AMPA. *Nature* **351**:745–748.

Fletcher EJ and Lodge D (1996) New developments in the molecular pharmacology of α-amino-3-hydroxy-5-methyl-4-isoxazole propionate and kainate receptors. *Pharmacol Ther* **70:**65–89.

Herb A, Burnashev N, Werner P, Sakmann B, and Sigworth FJ (1992) The KA-2 subunit of excitatory amino acid receptors shows widespread expression in brain and forms ion channels with distantly related subunits. *Neuron* **8:**775–785.

Hollmann M and Heinemann S (1994) Cloned glutamate receptors. *Annu Rev Neurosci* **17:**31–108.

Huettner JE (1990) Glutamate receptor channels in rat DRG neurons: Activation by kainate and quisqualate and blockade of desensitization by Con A. *Neuron* **5**:255–266.

Keinänen K, Wisden W, Sommer B, Werner P, Herb A, Verdoorn TA, Sakmann B, and Seeburg PH (1990) A family of AMPA-selective glutamate receptors. *Science (Washington DC)* **249:**556–560.

Keller BU, Blaschke M, Rivosecchi R, Hollmann M, Heinemann SF, and Konnerth A (1993) Identification of a subunit-specific antagonist of α-amino-3-hydroxy-5-methyl-4-isoxazolepropionate/kainate receptor channels. *Proc Natl Acad Sci USA* **90:**605–609.

Krogsgaard-Larsen P, Ferkany JW, Nielsen EØ, Madsen U, Ebert B, Johansen JS, Diemer NH, Bruhn T, Beattie DT, and Curtis DR (1991) Novel class of amino acid antagonists at non-*N*-methyl-D-aspartic acid excitatory amino acid receptors. Synthesis, in vitro and in vivo pharmacology, and neuroprotection. *J Med Chem* **34:**123–130.

Leff P and Dougall IG (1993) Further concerns over Cheng-Prusoff analysis. *Trends Pharmacol Sci* **14**:110–112.

Lew MJ and Angus JA (1995) Analysis of competitive agonist-antagonist interactions by nonlinear regression. *Trends Pharmacol Sci* **16:**328–337.

Madsen U, Bang-Andersen B, Brehm L, Christensen IT, Ebert B, Kristoffersen ITS,

Lang Y, and Krogsgaard-Larsen P (1996) Synthesis and pharmacology of highly selective carboxy and phosphono isoxazole amino acid AMPA receptor antagonists. *J Med Chem* **39:**1682–1691.
Meldrum BS (1994) The role of glutamate in epilepsy and other CNS disorders. *Neurology* **44**(suppl):14–23.
Nakanishi S and Masu M (1994) Molecular diversity and functions of glutamate receptors. *Annu Rev Biophys Biomol Struct* **23:**319–348.
Price CJ and Raymond LA (1996) Evans blue antagonizes both α-amino-3-hydroxy-5-methyl-4-isoxazolepropionate and kainate receptors and modulates receptor desensitization. *Mol Pharmacol* **50:**1665–1671.
Rogawski MA (1993) Therapeutic potential of excitatory amino acid antagonists: Channel blockers and 2,3-benzodiazepines. *Trends Pharmacol Sci* **14:**325–331.
Seeburg PH (1993) The TIPS/TINS lecture: The molecular biology of mammalian glutamate receptor channels. *Trends Pharmacol Sci* **14:**297–303.
Sheardown MJ, Nielsen EØ, Hansen AJ, Jacobsen P, and Honoré T (1990) 2,3-Dihydroxy-6-nitro-7-sulfamoylbenzo(*f*)quinoxaline. A neuroprotectant for cerebral ischemia. *Science (Washington DC)* **247:**571–574.
Simon RP, ed (1992) *Excitatory Amino Acids.* Thieme, New York.
Sommer B, Burnashev N, Verdoorn TA, Keinänen K, Sakmann B, and Seeburg PH (1992) A glutamate receptor channel with high affinity for domoate and kainate. *EMBO J* **11:**1651–1656.
Sommer B, Keinänen K, Verdoorn TA, Wisden W, Burnashev N, Herb A, Köhler M, Takagi T, Sakmann B, and Seeburg PH (1990) Flip and flop: A cell-specific functional switch in glutamate-operated channels of the CNS. *Science* **249:**1580–1585.
Traynelis SF and Wahl P (1997) Control of rat GluR6 glutamate receptor open probability by protein kinase A and calcineurin. *J Physiol* **503:**513–531.
Verdoorn, TA (1997) The functional diversity of native and recombinant AMPA receptors, in *The Ionotropic Glutamate Receptors* (Monaghan DT and Wenthold RJ, eds) pp 285–311, Humana Press, Totowa, NJ.
Wahl P, Nielsen B, Krogsgaard-Larsen P, Hansen JJ, Schousboe A, and Miledi R (1992) Stereoselective effects of AMOA on non-NMDA receptors expressed in *Xenopus* oocytes. *J Neurosci Res* **33**:392–397.
Watkins JC, Krogsgaard-Larsen P, and Honoré T (1990) Structure-activity relationships in the development of excitatory amino acid receptor agonists and competitive antagonists. *Trends Pharmacol Sci* **11:**25–33.
Wilding TJ and Huettner JE (1995) Differential antagonism of α-amino-3-hydroxy-5-methyl-4-isoxazolepropionic acid-preferring and kainate-preferring receptors by 2,3-benzodiazepines. *Mol Pharmacol* **47**:582–587.

Send reprint requests to: Philip Wahl, Ph.D., Department of Molecular Pharmacology, Novo Nordisk A/S, Novo Nordisk Park, DK 2760 Maaloev, Denmark. E-mail: pwa@novo.dk